Impaired clock output by altered connectivity in the circadian network

María de la Paz Fernández, Jessie Chu, Adriana Villella, Nigel Atkinson, Steve A. Kay, and María Fernanda Ceriani

PNAS published online Mar 16, 2007;
doi:10.1073/pnas.0608260104

Impaired clock output by altered connectivity in the circadian network

María de la Paz Fernández*, Jessie Chu†, Adriana Villella‡, Nigel Atkinson§, Steve A. Kay†, and María Fernanda Ceriani*¶

*Laboratorio de Genética del Comportamiento, Fundación Instituto Leloir, Av. Patricias Argentinas 435, 1405 Buenos Aires, Argentina; †Department of Biochemistry, The Scripps Research Institute, La Jolla, CA 92037; ‡Department of Biology, Brandeis University, Waltham, MA 02454; and §Department of Neurobiology, University of Texas, Austin, TX 78712-1064

Edited by Joseph S. Takahashi, Northwestern University, Evanston, IL, and approved February 12, 2007 (received for review September 21, 2006)

Substantial progress has been made in elucidating the molecular processes that impart a temporal control to physiology and behavior in most eukaryotes. In *Drosophila*, dorsal and ventral neuronal networks act in concert to convey rhythmicity. Recently, the hierarchical organization among the different circadian clusters has been addressed, but how molecular oscillations translate into rhythmic behavior remains unclear. The small ventral lateral neurons can synchronize certain dorsal oscillators likely through the release of pigment dispersing factor (PDF), a neuropeptide central to the control of rhythmic rest-activity cycles. In the present study, we have taken advantage of flies exhibiting a distinctive arrhythmic phenotype due to mutation of the potassium channel *slowpoke (slo)* to examine the relevance of specific neuronal populations involved in the circadian control of behavior. We show that altered neuronal function associated with the null mutation specifically impaired PDF accumulation in the dorsal protocerebrum and, in turn, desynchronized molecular oscillations in the dorsal clusters. However, molecular oscillations in the small ventral lateral neurons are properly running in the null mutant, indicating that *slo* is acting downstream of these core pacemaker cells, most likely in the output pathway. Surprisingly, disrupted PDF signaling by *slo* dysfunction directly affects the structure of the underlying circuit. Our observations demonstrate that subtle structural changes within the circadian network are responsible for behavioral arrhythmicity.

circadian circuitry | *Drosophila* | pigment dispersing factor | potassium channels | *slowpoke*

Rhythmicity in rest-activity cycles in *Drosophila* is under control of the circadian clock, which is based on self-sustaining, cell-autonomous transcriptional negative feedback loops. These feedback loops ultimately give rise to rhythms in the abundance, phosphorylation state, and nuclear localization of key intracellular proteins, such as period (PER) and timeless (TIM) (1). To date, several neuronal clusters have been shown to include a molecular oscillator. The one best understood encompasses the small ventral lateral neurons (LNvs), comprised of five cells, of which four rhythmically release the neuropeptide pigment dispersing factor (PDF) at their dorsal terminals. Other oscillators within the fly brain include the dorsal lateral neurons (LNds) together with the dorsal neurons (DN1–3) (2). Ablation of all LNvs by overexpression of proapoptotic genes, as well as null mutations on the *pdf* gene or its receptor, cause behavioral arrhythmicity a few days upon transfer to constant conditions (3–6) likely through the gradual loss of synchronization among the components of the small LNv cluster (7).

The question of how the intracellular molecular oscillations taking place within specific neuronal clusters ultimately drive rhythmic locomotor activity has only recently been approached in *Drosophila* (7–11). Molecular oscillations must be somehow transduced into neuronal function to generate a rhythm in behavior and physiology. Increasing evidence places electrical activity as an essential element in the propagation of such circadian oscillations. A possible mechanism to control membrane excitability is the circadian control of ion channel mRNA levels, which takes place in *Drosophila* (12, 13) and mammals (14). Free-running circadian rhythms in membrane conductance and K^+ channel current have been observed in pacemaker neurons of the molluscan retina (15, 16) and in mammals (17, 18). Alternatively, activation of second messenger cascades (such as calcium-dependent signaling) could also serve this purpose. In the suprachiasmatic nuclei cytoplasmic calcium levels have been shown to oscillate in a circadian manner (19, 20), with high calcium levels during the day and low levels at night, again serving as a possible link to control active membrane properties.

Drosophila slowpoke (*slo*) is the first voltage-gated calcium-dependent potassium channel of the "Big K" family to be cloned and characterized (21). A null mutation in the *slo* locus strikingly alters the electrical properties of both neurons and muscles (22–24), affecting neurotransmitter release (25) and thereby causing a variety of behavioral defects among those in courtship behavior (26–28). We have previously demonstrated that a *slo* null mutant is behaviorally arrhythmic under free-running [constant darkness (DD)] conditions (13). In the present work, we show that the loss of *slo* function in neuronal tissues is responsible for the highly arrhythmic phenotype. Whole-mount adult brain immunohistochemistry indicates that molecular oscillations are still intact in the small LNvs, whereas they are desynchronized in all dorsal clusters. Rhythmic PDF release is impaired in the null mutant in DD, thus explaining the lack of synchronicity between the ventral and dorsal oscillators. Remarkably, not only PDF levels, but also the proper arborization of the PDF terminals, are affected in the mutant. We propose that the electrical activity in the dorsal SLO+ clusters is impinging on the circadian control of the neuropeptide and the underlying PDF+ circuit, pointing to the SLO-expressing neurons as an intermediate relay circuit in the pathway relevant for rhythmic control of behavior.

Results

Lack of SLO Function in the CNS Accounts for Behavioral Arrhythmicity. *slo* is highly regulated at the transcriptional level, employing several alternative promoters and splice variants (29–31). To distinguish between a neuronal and/or a muscular defect associated with the strong impairment observed in *slo* mutants, we

Author contributions: M.d.l.P.F., S.A.K., and M.F.C. designed research; M.d.l.P.F., J.C., A.V., and M.F.C. performed research; N.A. contributed new reagents/analytic tools; M.d.l.P.F. and M.F.C. analyzed data; and M.F.C. wrote the paper.

The authors declare no conflict of interest.

This article is a PNAS direct submission.

Abbreviations: CT, circadian time; DD, constant darkness; DD3, 3 days after transfer to DD; DNs, dorsal neurons; LD, light–dark; LNds, dorsal lateral neurons; LNvs, ventral lateral neurons; PDF, pigment dispersing factor.

¶To whom correspondence should be addressed. E-mail: fceriani@leloir.org.ar.

This article contains supporting information online at www.pnas.org/cgi/content/full/0608260104/DC1.

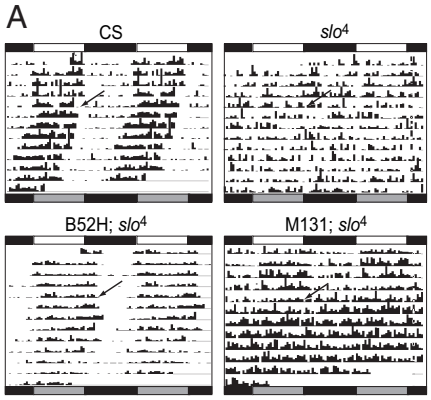

B

Genotype	n	LD	DD			Mean period, h	FFT
		%R	%R	%WR	%AR		
CS	68	96.1	85.3	8.8	5.9	23.69 ± 0.05	0.103 ± 0.005
slo^4	141	25.9	1.4	39.7	58.9	24.50 ± 0.50	0.049 ± 0.003
slo^1	48	60.0	55.0	30.0	15.0	24.00 ± 0.06	0.079 ± 0.004
M131;*slo*^{4}	50	10.4	1.2	15.6	83.2	24.25 ± 0.35	0.083 ± 0.007
B52H;*slo*^{4}	81	74.7	66.7	30.9	2.5	23.92 ± 0.04	0.090 ± 0.003
ash2^{18}/*slo*^{4}	49	30.2	14.2	62.9	22.8	23.60 ± 0.22	0.091 ± 0.056
ash2^{18}/+	15	100	100	0	0	23.77 ± 0.05	0.940 ± 0.083
slo^4/+	56	89.3	100	0	0	23.78 ± 0.40	0.117 ± 0.048

Fig. 1. Neuronal rescue of SLO function restores rhythmic rest-activity cycles. Newly eclosed males were synchronized and then released in DD (black arrow). Experiments were repeated three to nine times. (*A*) Representative double-plotted actograms from CS, *slo*^{4}, B52H;*slo*^{4}, and M131;*slo*^{4}. Open boxes, day; black boxes, night; gray boxes, subjective day. (*B*) Circadian phenotypes in various *slo* rescues. R, rhythmic; WR, weakly rhythmic; AR, arrhythmic. Period values were determined only on rhythmic individuals. The mean power Fast Fourier Transform (FFT) (a quantification of the strength of the rhythm) for those flies is shown. Statistical analysis included one-way ANOVA with the Bonferroni correction. *slo*^{4}, *ash2*^{18}/*slo*^{4}, and M131;*slo*^{4} are significantly different from CS ($P < 0.001$).

evaluated locomotor activity in two transgenic lines that rescue predominantly neuronal [B52H;*slo*^{4} (32)] or muscular [M131;*slo*^{4} (30)] defects associated with the lack of SLO. Wild-type flies entrain to light–dark (LD) cycles, consolidating their activity around the lights on/off transitions; under DD, a condition that allows the endogenous clock to manifest, flies are active throughout the subjective day, and the periodicity is usually close to, but not exactly, 24 h (Fig. 1*A*). On the contrary, *slo*^{4} is arrhythmic under DD (13). Restoring SLO activity with the muscular version did not change the degree of arrhythmicity under either condition (Fig. 1*B*). Conversely, the expression of the predominant neuronal version of *slo* under a noninduced constitutive promoter (B52H;*slo*^{4}) not only restored rhythmicity under LD, but, more importantly, it did so under DD (Fig. 1). This observation is further supported by the analysis of *ash2*^{18}/+ flies carrying a lethal inversion that exclusively removes the neural promoters away from the *slo* locus, leaving the remaining intact (33). This inversion has been shown to complement only the muscle-associated defects of *slo*^{4} (28). Fig. 1*B* shows that *ash2*^{18}/*slo*^{4} transheterozygotes were at best weakly rhythmic.

In summary, these results demonstrate that the *slo*^{4} locomotor phenotype is primarily due to altered electrical activity associated with the lack of SLO function in the neuronal circuits essential for clock-controlled behaviors.

SLO Expression in the Context of Circadian Structures. The severe arrhythmicity observed in *slo*^{4} suggests that SLO affects the activity of neuronal clusters controlling rhythmic behavior either by its presence in those specific neurons or in other cells connected to the same network. Becker *et al.* (29) reported adult *slo* expression in cortical regions of the optic lobe and central brain. We used a peptide antibody raised against the conserved C terminus of the *Periplaneta americana* channel (34) to map SLO to circadian-relevant structures. Immunohistochemistry on *tim-Gal4*/UAS-mCD8-GFP (*timGFP*; Fig. 2 *A–C*) and *pdf-Gal4*/UAS-mCD8-GFP (*pdfGFP*; Fig. 2 *D–F*) adult brains was performed. Although no DNs colocalized with SLO-reactive (SLO+) somas, we found a puncta-like SLO signal along the GFP+ projections of the dorsal neurons (Fig. 2 *B* and *C*, arrows). Most of the DNs extend their axons toward the *pars intercerebralis*, where a SLO+ cluster with large somata was found. Neither the small nor the large LNvs cell bodies expressed SLO. Instead, a strong signal adjacent to the small LNvs dorsal processes as well as to a number of PDF+ neurites projecting toward the optic lobe from the large LNvs was seen (Fig. 2 *D–F*). We also found an SLO-expressing cluster in the dorsal brain, precisely in the area where the small LNvs send their axonal projections (Fig. 2*F*). Although a presynaptic location of SLO would be consistent with a function in the control of transmitter release (25), the resolution of our micrographs do not allow us to unambiguously conclude whether SLO is effectively localized within the PDF dorsal projections. In any event, SLO cannot be restricted to these circadian clusters because restoring SLO expression by means of *pdf-Gal4* or *tim-Gal4* only partially rescued the *slo*^{4} phenotype (data not shown).

Recently, several laboratories reported the localization of the PDF receptor (4–6) with somewhat different results. Costaining analysis (Fig. 2*G*) highlighted that both SLO and PDRF displayed cell bodies (Fig. 2 *H* and *I*) and puncta along neuronal processes in the dorsal protocerebrum. Staining in projections along the main commissure and through the midline was especially intense (Fig. 2 *J* and *K*). Although the punctate nature of SLO and PDFR signals makes it difficult to assert whether they colocalize across the multiple projections observed, it is clear that both are present within a few clusters in the *pars lateralis* (Fig. 2*G*). This colocalization also supports a role for SLO in the output from the small LNvs. The nature of the SLO signal precludes a precise definition of whether it is present within the canonical circadian circuit. Yet SLO expression in neurons connected to it could still modify the electrical properties of the network, resulting in behavioral arrhythmicity.

Lack of Rhythmicity in *slo* Mutants Is Consistent with a Disrupted Output from Pacemaker Cells. *slo*^{4} flies displayed disrupted rest-activity and eclosion rhythmicity (data not shown) under DD. However, under 12:12-h LD cycles, a high proportion of *slo*^{4} individuals were weakly rhythmic and displayed a weak and delayed response to lights on instead of a "startle effect," the immediate behavioral response to the LD transitions that appears to be independent of an intact oscillator (35) [Fig. 1*B* and supporting information (SI) Fig. 6]. We then tested *slo*^{1}, another arrhythmic mutant (13), which has a relatively normal lights on response but lacks the ability to anticipate the night–day transition. Because the circadian anticipation to dawn and dusk largely overlaps with the startle effect under a 12:12-h LD regime, we chose to test a 16:8-h LD cycle following a 12:12-h entrainment (36) to better resolve these responses. Inspection of the average activity plots indicate that both wild type and *slo*^{4} displayed the lights on/off response as well as the evening peak; the latter became even more evident when evaluating *slo*^{1} (13),

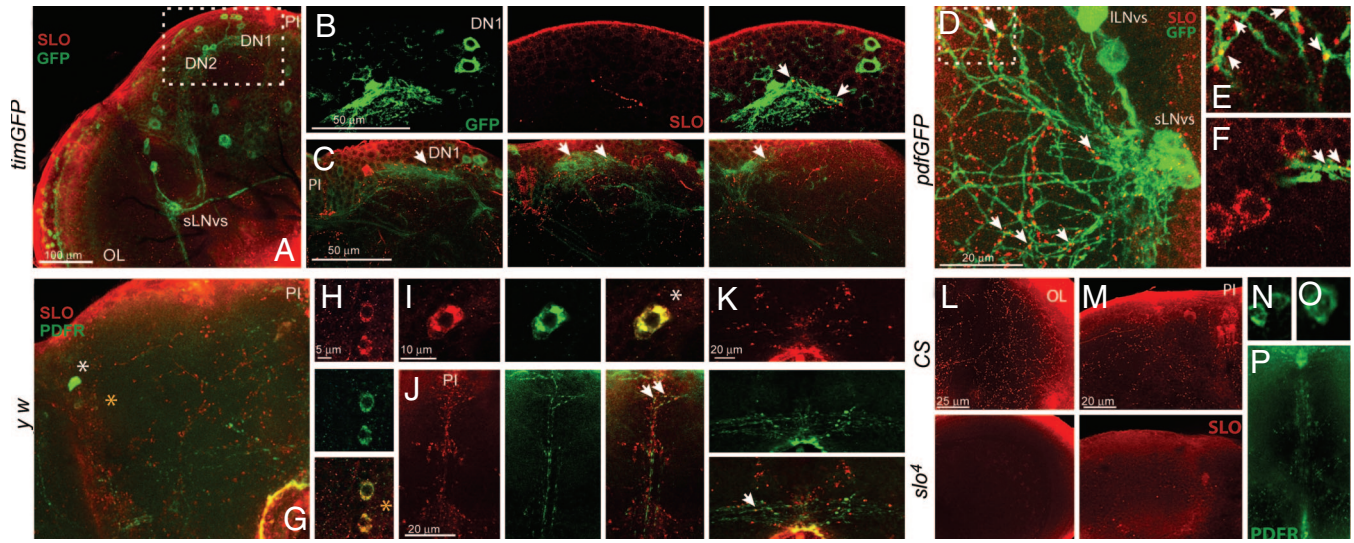

Fig. 2. SLO expression in the context of circadian structures. (*A–F*) *tim-Gal4*/UAS-CD8GFP (*timGFP*, *A–C*) and *pdf-Gal4*/UAS-CD8GFP (*pdfGFP*, *D–F*) brains were stained with anti GFP (green) and pSLO (red). Images with no label are the result of an overlay. Images shown in *A*, *D*, *G*, *L*, and *M* are projections, whereas the remaining ones are single optical scans. Arrows indicate colocalization. (*A*) SLO expression in a brain hemisphere displaying GFP+ *tim* neurons. (*B*) Inset from a dorsal region indicated in *A*, displaying axons from DNs juxtaposed to SLO+ neurites. (*C*) Inset from the same region of a different brain displaying three consecutive scans to illustrate how GFP+ axons reach a region where a cluster of SLO+ somas is located. (*D*) Extensive ramification of PDF and SLO+ neurites in the optic lobe. (*E*) Inset from *D* showing colocalization between both signals. (*F*) A higher magnification of a dorsalmost segment of the small LNvs projections from another brain showing SLO+ somas in the region where these PDF+ projections reach their targets. (*G–K*) Wild-type brains stained for PDFR (green) and SLO (red), revealing a widely distributed punctate signal. Symbols depict the anatomical regions from which the single focal planes were taken. Each image corresponds to a different brain. (*H* and *I*) Magnified views of a region similar to that indicated in *G*, revealing colocalization of SLO and PDFR in some of the cell bodies in which the two are expressed. (*J* and *K*) Images display punctate-like signal along the midline and the main commissure, respectively. (*L* and *M*) The specificity of the pSLO antibody was assessed comparing the signal in the optic lobe (*L*) and the dorsal area (*M*) between CS and *slo*^{4}. (*N–P*) PDFR signal in *slo*^{4} brains in the regions shown in *H–J*, respectively.

clearly indicating that this circadian-controlled behavior was unaffected in the mutant (SI Fig. 6*B*). However, only wild-type flies displayed a morning peak (SI Fig. 6*A*), suggesting that the molecular oscillators sustaining the morning and evening components of the rest-activity pattern under synchronized conditions were distinctly affected by the lack of *slo* function, which is also consistent with an impaired output from the central pacemaker cells (8, 9).

Molecular Oscillations Are Preserved in *slo*^{4} Pacemaker Cells. Abnormal excitability and firing pattern in the circuits underlying rhythmic behavior could alter the core molecular oscillations (37) and serve to explain the lack of rhythmicity observed in *slo*^{4}. To directly assess the pace of the intracellular molecular clock, whole-mount brain immunohistochemistry was carried out to monitor PER and TIM subcellular distribution in the small LNvs. Interestingly, *slo*^{4} samples were undistinguishable from Canton S (CS) throughout time courses performed in LD and 3 days after transfer to DD (DD3) (data not shown and Fig. 3, respectively). In the small LNvs of CS and *slo*^{4}, PER was found in the nucleus at CT5 and CT11. By CT17, intense cytoplasmic PER was detected, although a mild nuclear signal could be seen. At CT23, PER protein was exclusively located within the nucleus. In contrast, TIM was undetectable until CT17, when it was mainly located in the cytoplasm, and it became nuclear by CT23. Remarkably, no differences were detected in the pace of these

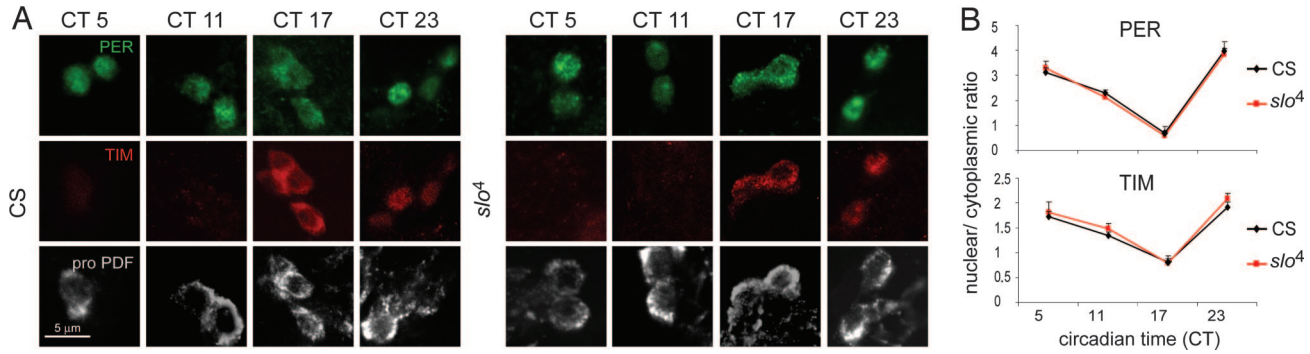

Fig. 3. Molecular oscillations in pacemaker neurons are not affected in *slo*^{4}. Newly eclosed CS and *slo*^{4} adult flies were synchronized, and samples were taken in DD3. Whole-mount brain immunohistochemistry was performed to follow TIM (red) or PER (green) and proPDF (white) accumulation at CT5, CT11, CT17, and CT23. A minimum of 12 brains per genotype were analyzed at each time point. (*A*) Representative confocal stacks focused on the small LNvs in wild-type flies (*Left*) and *slo*^{4} (*Right*). Time courses were analyzed blind and repeated three to five times with identical results. (*B*) Ratio between nuclear and cytoplasmic PER/TIM signal. Error bars represent the SE of the mean. No statistical differences were found between both genotypes ($P > 0.05$). See *Materials and Methods* for details on quantitation methods and statistics.

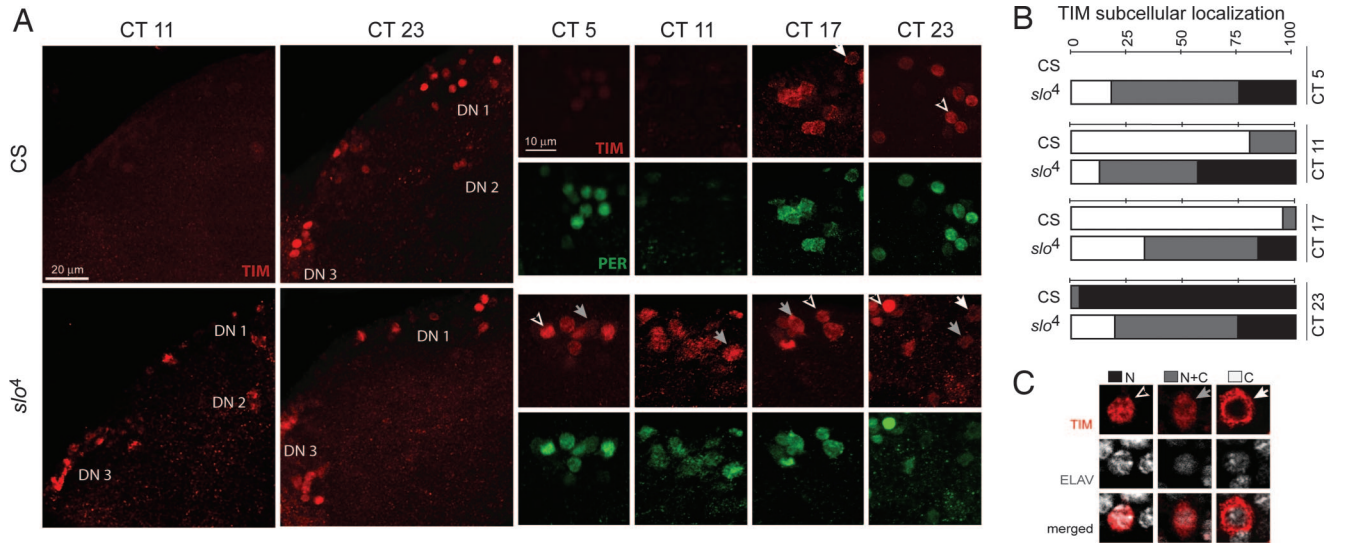

Fig. 4. Dorsal clusters are out of phase in the absence of synchronizing signals. (*A*) (*Right*) Whole-mount brain immunocytochemistry on the DN1 region of CS and *slo*^{4} flies taken in DD3 at CT5, CT11, CT17, and CT23 stained for TIM (red), PER (green), and ELAV (data not shown). Results were consistent in the brains (n = 7–21) analyzed at each time point in 2–4 experiments. (*Left*) Representative images of low magnification at CT11 and CT23. (*B*) Quantitation of TIM distribution in DN1s. Black bars, nuclear (N); white bars, cytoplasmic (C); gray bars, nonlocalized (N + C) TIM signal. χ^2 analysis of the frequency distribution retrieved a significantly different distribution throughout the time course between CS and *slo*^{4} brains ($P < 0.0001$). Between 4–12 DN1 cells could be counted at each time point. Lack of TIM signal in CS flies at CT5 reflects that most brains showed no TIM, and those that did were dim enough to forfeit any attempt of localization. (*C*) Example of how localization was assessed: C, absence of colocalization with ELAV (white arrows); N, absolute colocalization of both signals (black arrows); N + C (or nonlocalized), cells where the signal could not be attributed to any single compartment (gray arrows).

molecular oscillations between both genotypes (Fig. 3*B*), which stayed undistinguishable even after 8 days in DD, suggesting that the defect resulting in the arrhythmic phenotype lies downstream of this oscillator (SI Fig. 7*A*).

We used a transgenic line that expresses the *luc* reporter under the control of the *tim* promoter as an independent assessment of the molecular oscillations. This transgenic line allows monitoring clock function in real time, and recorded oscillations derive from most tissues scattered throughout the fly. Under this paradigm, both wild type and *slo*^{4} displayed rhythmic *luc* oscillations, with a comparable phase and amplitude in LD and DD cycles (SI Fig. 7*B*), strongly suggesting that molecular peripheral clocks are running in phase in the absence of SLO function.

Molecular Oscillations Are Disrupted in Dorsal Circuits. Given the pervasive arrhythmic phenotype of *slo*^{4}, we wondered whether the molecular oscillations could be impaired in any of the dorsal oscillators in the adult fly brain. We performed time courses to evaluate PER/TIM oscillations under entrained and free-running conditions. A nuclear label (anti-ELAV) was used to determine whether PER/TIM cycled between subcellular compartments as well as in abundance in these clusters. Newly eclosed CS and *slo*^{4} flies were entrained, and samples were taken in either LD or DD3. Under LD, PER/TIM displayed an identical distribution in the DN1s and LNds of both strains, and, more importantly, this localization mirrored what had been seen in the small LNvs (data not shown).

However, both DN1 and LNds were also analyzed at CT5, CT11, CT17, and CT23 on DD3. In wild-type DN1s (Fig. 4) and LNds (see SI Fig. 8), TIM was usually absent at CT5, primarily cytoplasmic at CT11, and highly concentrated within the cytoplasm by CT17. At CT23, TIM was found almost entirely in the nucleus in wild-type brains (Fig. 4*A*). In contrast, low levels of nuclear PER were detected in the subjective morning (CT5) and became barely detected by CT11; later on PER was found primarily cytoplasmic by CT17 and back into the nucleus at CT23. In contrast, a mixed population was evidenced within the DN1 and LNds in *slo*^{4}; in fact, TIM could be found in the nucleus, cytoplasm, or a more ubiquitous localization within a cluster in a particular *slo*^{4} hemisphere at any given time point (Fig. 4*B* and SI Fig. 8*B*), underscoring the lack of synchronization within these cells. Expression of neuronal SLO rescued PER and TIM molecular oscillations in both clusters in DD3 (data not shown).

These results suggest that lack of SLO function is responsible for the impairment of dorsal oscillations affecting the connection between ventral and dorsal clusters, presumably through the disruption of PDF signaling (7, 38, 39).

PDF Accumulation Is Impaired in *slo* Mutants. Most of the defects associated with the lack of SLO function in *slo*^{4} are commensurate with an impaired output from the small LNvs. Because PDF is the only factor known to be involved in this process, we characterized the PDF neurons and their projections in detail. The neurons' integrity appeared to be well preserved, that is, somatas were properly located and their projections did not appear to show any defects (Fig. 5*A Left*). However, we noticed a stark difference at the level of the axonal termini of the projections running toward the dorsal protocerebrum, in which PDF levels have been reported to be circadianly controlled (40). In wild-type flies, the PDF signal appeared to be more widespread (and intense) in the early day than at night, both under LD and DD. In contrast, *slo*^{4} displayed a reduced PDF signal throughout the day, more reminiscent of what is seen in wild-type brains at night (Fig. 5*A Right*). Moreover, the axonal projections remained tightly fasciculated throughout the entire path and did not show evenly spaced varicosities as in wild-type brains, but they did show a very prominent and contiguous PDF signal (Fig. 5*A Right Inset*). These data indicated that loss of SLO function affects PDF accumulation or release in the fly brain.

To corroborate detection of the PDF arborizations independently of the neuropeptide accumulation, we used a *pdf*-Gal4/UAS-mCD8-GFP line (Fig. 5*C*). We looked for the dorsal thinner projections in wild-type brains at the time of day when the axonal arbor is at its maximum, and we found that GFP and

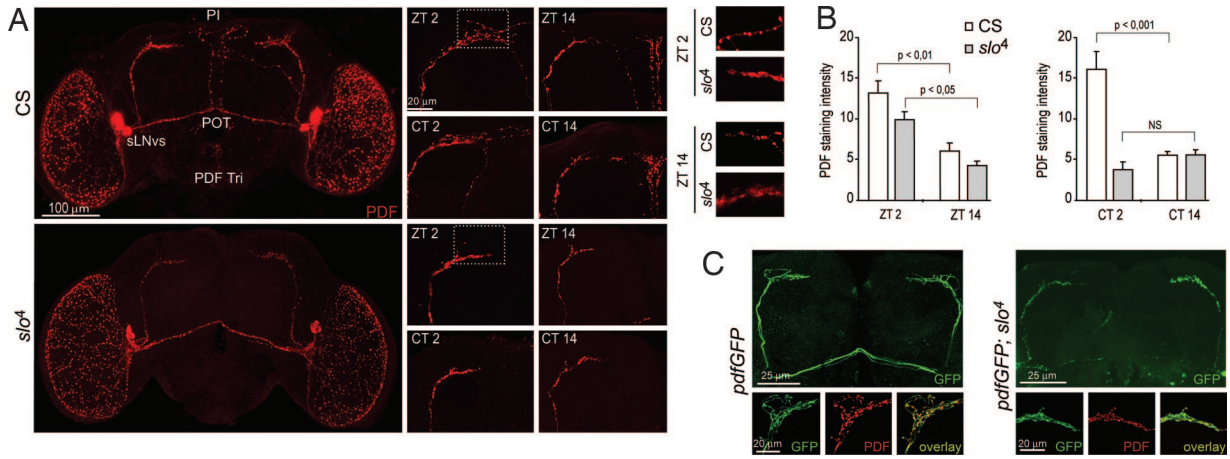

Fig. 5. Mutation in *slo* affects normal axonal arborization of pacemaker cells. (*A*) (*Left*) PDF secretion or accumulation is altered in *slo*^{4}. Whole-mount brain immunohistochemistry of CS and *slo*^{4} flies stained for PDF. Brains <1 day old were fixed at the times indicated in the figure (CT samples were taken on DD2). Experiments were repeated at least three times, and a minimum of 50 brains were analyzed per time point. (*Right*) Magnified views of the PDF+ projections in the dorsal region. Box shows the area quantified in *B*. PI, *pars intercerebralis*; POT, posterior optic tract. (*B*) Quantitation of the average intensity of the LNvs dorsal projections. Error bars represent the SE of the mean. No circadian differences in PDF intensity in *slo*^{4} were found ($P > 0.05$). See *Materials and Methods* for details on quantitation methods and statistics. (*C*) (*Upper*) Evaluation of the structure of the PDF projections in *pdfGFP* and *pdfGFP;slo*^{4} flies stained for PDF (red) and GFP (green). (*Lower*) Higher magnification view of the dorsalmost segment.

PDF signals colocalized throughout the circuit and the PDF+ puncta were contained within GFP-labeled membranes of the dorsal termini. Strikingly, in *pdfGFP;slo*^{4} brains, both the PDF and GFP signals colocalized, indicating that loss of SLO function not only affected the accumulation of the neuropeptide, but also altered the axonal arborization of the PDF+ neurons (Fig. 5*C*).

Therefore, loss of SLO function specifically affected PDF axonal arborization, preventing a proper synchronization of the circadian network, and thus impacted on rhythmic behavior.

Discussion

Lack of Neuronal SLO Correlates with the Arrhythmic Behavior. We previously demonstrated that a null mutation in a clock-controlled gene that encodes the calcium-dependent voltage-gated potassium channel *slo* gives rise to a highly arrhythmic locomotor behavior phenotype (13). In the present work, we extended these original observations by using a transgenic line that expresses the most prevalent neuronal SLO version throughout the brain and has been shown to rescue other neuronal deficits of *slo*^{4} (32) to demonstrate that it is the lack of channel activity in CNS neurons that gives rise to the full phenotype (Fig. 1). Employing different entraining paradigms, we ruled out an inability to respond to light as the major component for the arrhythmicity (SI Fig. 6).

The Defect Lies Downstream of Pacemaker Function. The lack of rhythmicity characteristic of *slo*^{4} could derive from an abnormal core oscillator function, which would manifest at the level of the central pacemaker neurons and other peripheral tissues. We first investigated molecular oscillations in the small LNvs because their hierarchy over other brain oscillators in the rhythmic control of locomotor behavior is well documented (9, 10, 41, 42). We monitored PER and TIM oscillations on whole-mount brains and found neither changes in subcellular localization nor differences between the amplitude of the rhythmic oscillations in the *slo*^{4} background compared with wild-type controls (Fig. 3 and SI Fig. 7). These results clearly indicate that, regardless of the nature of the arrhythmicity, lack of SLO does not affect the underpinnings of the self-sustained molecular clock in every cell. Moreover, despite the potential defects in the excitability of the underlying circuits in *slo*^{4}, no alterations or rundown of the molecular oscillations in pacemaker cells were evidenced (37, 43).

Lack of SLO Function Differentially Affects Dorsal Oscillators Under Free-Running Conditions. Not surprisingly, given that most circadian structures are light-responsive per se, no difference was observed between CS and *slo*^{4} when the pace of the oscillations in dorsal clusters was evaluated in LD, suggesting that they are not directly responsible for the weak rhythmicity of the rest-activity cycles in *slo*^{4}. However, when molecular oscillations were evaluated under free-running conditions, a lack of synchronization was detected between the ventral and dorsal clusters (Fig. 4 and SI Fig. 8), in contrast to what has been reported for a null mutant in the channel narrow abdomen (44). Our data strongly suggest that dorsal oscillators are clearly taking part in the circuitry behind rhythmic control of rest-activity cycles under free-running conditions as previously suggested (38), and the hierarchy of the small LNvs is most likely exerted through the release of PDF at the dorsal terminals.

Abnormal PDF Projections Account for Lack of Rhythmicity Under Free-Running Conditions. *slo*^{4} mutants appeared to have intact PDF neurons. However, the dorsal projections toward the *pars intercerebralis* were clearly disrupted (Fig. 5 *A* and *B*). We hypothesized that the pervasive arrhythmicity observed in this mutant was linked to the absence of proper PDF processes. We then evaluated its integrity in the neuronal rescue (B52H;*slo*^{4}) and found that most brains showed strong PDF labeling (data not shown). Thus, distorted electrical activity in *slo*^{4} mutant flies is likely responsible for the abnormal PDF release and/or accumulation.

We also provide evidence that loss of SLO function altered the degree of axonal arborization within that region (Fig. 5 *A Inset* and *C*). Labeling the PDF-expressing neurons by independent means (*pdfGFP;slo*^{4}) showed no gross anatomical changes in *slo*^{4}. That the lack of SLO function affects the connectivity of the PDF neurons suggests that its function is relevant in related circuits whose activity affects the maintenance or plasticity of PDF+ oscillators (or both). In any case, the observation that dorsal SLO neurons could potentially receive synaptic connections from projections of both ventral and dorsal oscillators (Fig. 2 *C* and *F*) strongly suggests that the dorsal SLO-expressing neurons are indeed part of the network required for rhythmic behavior.

Does the Lack of PDF Account for the *slo*^{4} Phenotype? Consistent with our hypothesis that the impact of the lack of neuronal SLO on rhythmic behavior is a consequence of the down-regulation of the synchronizing PDF signal, the *slo*^{4} phenotype is reminiscent of that of the *pdf*^{0} flies under free-running conditions. In DD, ≈70% of the *pdf*^{0} flies gradually lose rhythmicity, and the remainder displays only weak rhythms (3). Recently, PDF has been proposed to coordinate the phase and amplitude of molecular rhythms among diverse pacemaker cells (7, 10, 39), which is consistent with our observation that lack of dorsomedial PDF signal correlated with altered molecular oscillations within the dorsal brain. Although *pdf*^{0} are rhythmic and anticipate the evening transition under standard entraining conditions (3, 7), such properties only become evident under extended photoperiod in *slo*^{4}, revealing additional aspects of behavioral control that are altered in the absence of SLO function.

In summary, these data establish that the network underlying rhythmic rest-activity cycles depends on the function of Ca^{2+}-dependent voltage-gated potassium channels of the Big K family such as SLO, whose transcription is under clock control in both *Drosophila* (13) and mammals (14, 45). More importantly, lack of SLO function directly impinges on the fine-tuning of the circuit underlying this rhythmic behavior. Perhaps not surprisingly, it has recently been reported that a Big K null mice display disorganized rhythms in locomotor activity while rendering intact the molecular oscillations in the SCN (45), underscoring the degree of conservation between flies and mammals.

Materials and Methods

Detailed protocols are shown in *SI Methods*.

Strains and Fly Rearing. CS flies were used as wild-type controls. *slo*^{4}, B52H;*slo*^{4}, M131;*slo*^{4}, and *ash2*^{18} were previously described (21, 30, 33).

Behavioral Analyses. Fly activity was monitored under LD conditions for 5 days when flies were released into DD at least for 1 week as in ref. 13.

Immunohistochemistry and Imaging. Synchronized 1- to 5-day-old flies were used. Immunohistochemistry was performed essentially as in ref. 46. Whole-mount brains were imaged on a Zeiss LSM510 confocal microscope (Carl Zeiss, Thornwood, NJ). Statistical analysis was performed employing the Prism Graphpad 4.0 software package (San Diego, CA).

We thank A. Schinder and L. Centanin for invaluable discussions; A.S.R. Fitzsimonds, J. Berni, and C. Rezával for critical reading of the manuscript; J. Hall, F. Rouyer, P. Taghert, M. Young, M. Rosbash, and D. Wicher for various antibodies; and the Bloomington Stock Center (Bloomington, IN) for fly stocks. The elav-9F8A9 antibody was obtained from the Developmental Studies Hybridoma Bank. This work was supported by the Fogarty International Research Collaboration Award R03TW005998-01 (to S.A.K. and M.F.C.) and the Howard Hughes Medical Institute International Research Program 55003668 (to M.F.C.). M.F.C. is a member of the National Research Council (CONICET), a Howard Hughes Medical Institute International Scholar, and held reentry grants from the Argentine Ministry of Health, the PEW Charitable Trust, and Fundación Antorchas. M.d.l.P.F. is supported by a graduate fellowship from National Research Council. This is manuscript no. 18765 for The Scripps Research Institute.

1. Hardin PE (2005) *Curr Biol* 15:R714–R722.
2. Shafer OT, Helfrich-Forster C, Renn SC, Taghert PH (2006) *J Comp Neurol* 498:180–193.
3. Renn SC, Park JH, Rosbash M, Hall JC, Taghert PH (1999) *Cell* 99:791–802.
4. Lear BC, Merrill CE, Lin JM, Schroeder A, Zhang L, Allada R (2005) *Neuron* 48:221–227.
5. Mertens I, Vandingenen A, Johnson EC, Shafer OT, Li W, Trigg JS, De Loof A, Schoofs L, Taghert PH (2005) *Neuron* 48:213–219.
6. Hyun S, Lee Y, Hong ST, Bang S, Paik D, Kang J, Shin J, Lee J, Jeon K, Hwang S, *et al.* (2005) *Neuron* 48:267–278.
7. Lin Y, Stormo GD, Taghert PH (2004) *J Neurosci* 24:7951–7957.
8. Stoleru D, Peng Y, Agosto J, Rosbash M (2004) *Nature* 431:862–868.
9. Grima B, Chelot E, Xia R, Rouyer F (2004) *Nature* 431:869–873.
10. Stoleru D, Peng Y, Nawathean P, Rosbash M (2005) *Nature* 438:238–242.
11. Nitabach MN, Wu Y, Sheeba V, Lemon WC, Strumbos J, Zelensky PK, White BH, Holmes TC (2006) *J Neurosci* 26:479–489.
12. Claridge-Chang A, Wijnen H, Naef F, Boothroyd C, Rajewsky N, Young MW (2001) *Neuron* 32:657–671.
13. Ceriani MF, Hogenesch JB, Yanovsky M, Panda S, Straume M, Kay SA (2002) *J Neurosci* 22:9305–9319.
14. Panda S, Antoch MP, Miller BH, Su AI, Schook AB, Straume M, Schultz PG, Kay SA, Takahashi JS, Hogenesch JB (2002) *Cell* 109:307–320.
15. Michel S, Geusz ME, Zaritsky JJ, Block GD (1993) *Science* 259:239–241.
16. Michel S, Manivannan K, Zaritsky JJ, Block GD (1999) *J Biol Rhythms* 14:141–150.
17. Kuhlman SJ, McMahon DG (2004) *Eur J Neurosci* 20:1113–1117.
18. Pitts GR, Ohta H, McMahon DG (2006) *Brain Res* 1071:54–62.
19. Colwell CS (2000) *Eur J Neurosci* 12:571–576.
20. Ikeda M, Sugiyama T, Wallace CS, Gompf HS, Yoshioka T, Miyawaki A, Allen CN (2003) *Neuron* 38:253–263.
21. Atkinson NS, Robertson GA, Ganetzky B (1991) *Science* 253:551–555.
22. Elkins T, Ganetzky B (1988) *J Neurosci* 8:428–434.
23. Elkins T, Ganetzky B, Wu CF (1986) *Proc Natl Acad Sci USA* 83:8415–8419.
24. Saito M, Wu CF (1991) *J Neurosci* 11:2135–2150.
25. Warbington L, Hillman T, Adams C, Stern M (1996) *Invert Neurosci* 2:51–60.
26. Peixoto AA, Hall JC (1998) *Genetics* 148:827–838.
27. Brenner R, Yu JY, Srinivasan K, Brewer L, Larimer JL, Wilbur JL, Atkinson NS (2000) *J Neurochem* 75:1310–1319.
28. Atkinson NS, Brenner R, Chang W, Wilbur J, Larimer JL, Yu J (2000) *J Neurosci* 20:2988–2993.
29. Becker MN, Brenner R, Atkinson NS (1995) *J Neurosci* 15:6250–6259.
30. Atkinson NS, Brenner R, Bohm RA, Yu JY, Wilbur JL (1998) *Ann NY Acad Sci* 860:296–305.
31. Brenner R, Thomas TO, Becker MN, Atkinson NS (1996) *J Neurosci* 16:1827–1835.
32. Ghezzi A, Al Hasan YM, Larios LE, Bohm RA, Atkinson NS (2004) *Proc Natl Acad Sci USA* 101:17276–17281.
33. Adamson AL, Shearn A (1996) *Genetics* 144:621–633.
34. Derst C, Messutat S, Walther C, Eckert M, Heinemann SH, Wicher D (2003) *Eur J Neurosci* 17:1197–1212.
35. Wheeler DA, Hamblen-Coyle MJ, Dushay MS, Hall JC (1993) *J Biol Rhythms* 8:67–94.
36. Rieger D, Stanewsky R, Helfrich-Forster C (2003) *J Biol Rhythms* 18:377–391.
37. Nitabach MN, Blau J, Holmes TC (2002) *Cell* 109:485–495.
38. Peng Y, Stoleru D, Levine JD, Hall JC, Rosbash M (2003) *PLoS Biol* 1:E13.
39. Klarsfeld A, Malpel S, Michard-Vanhee C, Picot M, Chelot E, Rouyer F (2004) *J Neurosci* 24:1468–1477.
40. Park JH, Helfrich-Forster C, Lee G, Liu L, Rosbash M, Hall JC (2000) *Proc Natl Acad Sci USA* 97:3608–3613.
41. Helfrich-Forster C (1998) *J Comp Physiol A* 182:435–453.
42. Blanchardon E, Grima B, Klarsfeld A, Chelot E, Hardin PE, Preat T, Rouyer F (2001) *Eur J Neurosci* 13:871–888.
43. Nitabach MN, Sheeba V, Vera DA, Blau J, Holmes TC (2005) *J Neurobiol* 62:1–13.
44. Lear BC, Lin JM, Keath JR, McGill JJ, Raman IM, Allada R (2005) *Neuron* 48:965–976.
45. Meredith AL, Wiler SW, Miller BH, Takahashi JS, Fodor AA, Ruby NF, Aldrich RW (2006) *Nat Neurosci* 9:1041–1049.
46. Rezával C, Werbajh S, Ceriani MF (2007) *Eur J Neurosci* 25:683–694.